The Transpolar Drift as a Source of Riverine and Shelf-Derived Trace Elements to the Central Arctic Ocean

Matthew A Charette, Lauren Kipp, Laramie Jensen, Jessica Dabrowski, Laura Whitmore, Jessica Fitzsimmons, Tatiana Williford, Adam Ulfsbo, Elizabeth Jones, Randelle Bundy, et al.

Paper 'The Transpolar Drift as a Source of Riverine and Shelf-Derived Trace Elements to the Central Arctic Ocean'

Matthew A. Charette[*1], Lauren E. Kipp[2,3], Laramie T. Jensen[4], Jessica S. Dabrowski[1], Laura M. Whitmore[5], Jessica N. Fitzsimmons[4], Tatiana Williford[4], Adam Ulfsbo[6], Elizabeth Jones[7], Randelle M. Bundy[1,8], Sebastian M. Vivancos[3,9], Katharina Pahnke[10], Seth G. John[11], Yang Xiang[12], Mariko Hatta[13], Mariia V. Petrova[14], Lars-Eric Heimbürger-Boavida[14], Dorothea Bauch[15], Robert Newton[3], Angelica Pasqualini[3], Alison M. Agather[16], Rainer M.W. Amon[4,17], Robert F. Anderson[3], Per S. Andersson[18], Ronald Benner[19], Katlin L. Bowman[12], R. Lawrence Edwards[20], Sandra Gdaniec[18,21,22], Loes J.A. Gerringa[23], Aridane G. González[24,25], Mats Granskog[26], Brian Haley[27], Chad R. Hammerschmidt[16], Dennis A. Hansell[28], Paul B. Henderson[1], David C. Kadko[29], Karl Kaiser[4,17], Phoebe J. Lam[12], Carl H. Lamborg[12], Martin Levier[22], Xianglei Li[20], Andrew R. Margolin[28,30], Chris Measures[13], Frank J. Millero[28], Willard S. Moore[19], Ronja Paffrath[10], Hélène Planquette[24], Benjamin Rabe[31], Heather Reader[32,33], Robert Rember[34], Micha J.A., Rijkenberg[23], Matthieu Roy-Barman[22], Michiel Rutgers van der Loeff[31], Mak Saito[1], Ursula Schauer[31], Peter Schlosser[3], Robert M. Sherrell[35,36], Alan M. Shiller[5], Hans Slagter[23,37], Jeroen E. Sonke[38], Colin Stedmon[32], Ryan J. Woosley[28,39], Ole Valk[31], Jan van Ooijen[23], Ruifeng Zhang[11,40]

*corresponding author, mcharette@whoi.edu, +001-508-289-3205

1. Woods Hole Oceanographic Institution, Woods Hole, MA USA
2. Dalhousie University, Halifax, NS, Canada
3. Lamont-Doherty Earth Observatory of Columbia University, Palisades, NY, USA
4. Department of Oceanography, Texas A&M University, College Station, TX, USA
5. School of Ocean Science and Engineering, University of Southern Mississippi, Stennis Space Center, MS, USA

6. Department of Marine Sciences, University of Gothenburg, Gothenburg, Sweden.
7. Institute of Marine Research, Fram Centre, Tromsø, Norway
8. School of Oceanography, University of Washington, Seattle, Washington, USA
9. Department of Earth and Environmental Sciences, Columbia University, New York, NY, USA
10. Institute for Chemistry and Biology of the Marine Environment (ICBM), University of Oldenburg, Carl-von-Ossietzky-Str. 9-11, 26129 Oldenburg, Germany
11. Department of Earth Sciences, University of Southern California, Los Angeles, CA USA
12. Department of Ocean Sciences, University of California, Santa Cruz, Santa Cruz, CA, USA
13. Department of Oceanography, University of Hawaii at Manoa, 1000 Pope Road, Honolulu, Hawaii, USA
14. Aix Marseille Université, CNRS/INSU, Université de Toulon, IRD, Mediterranean Institute of Oceanography (MIO), UM 110, F-13288 Marseille, France
15. GEOMAR Helmholtz Center for Ocean Research Kiel, 24148 Kiel, Germany
16. Department of Earth and Environmental Sciences, Wright State University, Dayton, OH, USA
17. Department of Marine Science, Texas A&M University at Galveston, Texas, USA
18. Swedish Museum of Natural History, Department of Geosciences, Stockholm, Sweden
19. School of the Earth, Ocean and Environment, University of South Carolina, Columbia, SC, USA
20. Department of Earth and Environmental Sciences, University of Minnesota, Minneapolis, MN USA
21. Stockholm University, Department of Geological Sciences, Stockholm, Sweden
22. Laboratoire des Sciences du Climat et de l'Environnement, LSCE/IPSL, CEA-CNRS-UVSQ, Université Paris-Saclay, Gif-sur-Yvette, France
23. Department of Ocean Systems, NIOZ Royal Institute for Sea Research and Utrecht University, Den Burg, Netherlands

24. University of Brest, CNRS, IRD, Ifremer, LEMAR, F-29280 Plouzané, France
25. Instituto de Oceanografía y Cambio Global, IOCAG, Universidad de Las Palmas de Gran Canaria, ULPGC, Las Palmas de Gran Canaria (ULPGC), Las Palmas, Spain
26. Norwegian Polar Institute, Tromsø, Norway
27. College of Earth, Ocean, and Atmospheric Sciences, Oregon State University, Corvalis, OR, USA
28. Rosenstiel School of Marine and Atmospheric Science, University of Miami, Miami, FL, USA
29. Florida International University, Applied Research Center, Miami, FL, USA
30. Institute for the Oceans and Fisheries, University of British Columbia, Vancouver, British Columbia, Canada
31. Alfred-Wegener-Institut Helmholtz-Zentrum für Polar- und Meeresforschung, Bremerhaven, Germany
32. Technical University of Denmark, National Institute of Aquatic Resources, Lyngby Denmark
33. Department of Chemistry, Memorial University of Newfoundland, St John's, NL, Canada
34. International Arctic Research Center, University of Alaska, Fairbanks, Fairbanks, AK, USA
35. Department of Marine and Coastal Sciences, Rutgers University, New Brunswick, NJ, USA
36. Department of Earth and Planetary Sciences, Rutgers University, Piscataway, NJ, USA
37. Max Planck Institute for Chemistry, Mainz, Germany
38. Laboratoire Géosciences Environnement Toulouse, CNRS/Institute for Research and Development/Université Paul Sabatier–Toulouse III, 31400 Toulouse, France
39. Center for Global Change Science, Massachusetts Institute of Technology, Cambridge, MA, USA
40. School of Oceanography, Shanghai Jiao Tong University, Shanghai, China

Key Points

- The Transpolar Drift is a source of shelf- and river-derived elements to the central Arctic Ocean
- The TPD is rich in dissolved organic matter (DOM), which facilitates long-range transport of trace metals that form complexes with DOM
- Margin trace element fluxes may increase with future Arctic warming due to DOM release from permafrost thaw and increasing river discharge

Abstract

A major circulation feature of the Arctic Ocean is the Transpolar Drift (TPD), a surface current that transports river-influenced shelf water from the Laptev and East Siberian Seas toward the central basin and Fram Strait. In 2015, the international GEOTRACES program included a high-resolution pan-Arctic survey of carbon, nutrients, and a suite of trace elements and isotopes (TEIs). The cruises bisected the TPD at two locations in the central basin, which was defined by maxima in meteoric water and dissolved organic carbon concentrations that spanned 600 km horizontally and ~25-50 m vertically. Dissolved TEIs such as Fe, Co, Ni, Cu, Hg, Nd, and Th, which are generally particle-reactive but can be complexed by organic matter, were observed at concentrations much higher than expected for the open ocean setting. Other trace element concentrations such as Al, V, Ga, and Pb were lower than expected due to scavenging over the productive eastern Arctic shelves. Using a combination of radionuclide tracers and ice drift modeling, the transport rate for the core of the TPD was estimated at 0.9 ± 0.4 Sv (10^6 m^3 s^{-1}). This rate was used to derive the mass flux for TEIs that were enriched in the TPD, revealing the importance of lateral transport in supplying materials beneath the ice to the central Arctic Ocean and potentially to the North Atlantic Ocean *via* Fram Strait. Continued intensification of the Arctic hydrologic cycle and permafrost degradation will likely lead to an increase in the flux of TEIs into the Arctic Ocean.

Keywords

Arctic Ocean, Transpolar Drift, trace elements, carbon, nutrients, GEOTRACES

Plain Language Summary

A major feature of the Arctic Ocean circulation is the Transpolar Drift (TPD), a surface current that carries ice and continental shelf-derived materials from Siberia across the North Pole to the North Atlantic Ocean. In 2015, an international team of oceanographers conducted a survey of trace elements in the Arctic Ocean, traversing the TPD. Near the North Pole, they observed much higher concentrations of trace elements in surface waters than in regions on either side of the current. These trace elements originated from land and their journey across the Arctic Ocean is made possible by chemical reactions with dissolved organic matter that originates mainly in Arctic rivers. This study reveals the importance of rivers and shelf processes combined with strong ocean currents in supplying trace elements to the central Arctic Ocean and onwards to the Atlantic. These trace element inputs are expected to increase as a result of permafrost thawing and increased river runoff in the Arctic, which is warming at a rate much faster than anywhere else on Earth. Since many of the trace elements are essential building blocks for ocean life, these processes could lead to significant changes in the marine ecosystems and fisheries of the Arctic Ocean.

Introduction

Of all the major oceans on Earth, the Arctic Ocean is the most heavily influenced by processes occurring over continental shelves, which cover over 50% of its area (Jakobsson, 2002). The Arctic Ocean also has the lowest salinity surface waters, a result of limited evaporation, high riverine inputs, the annual sea-ice freeze/melt cycle, and restricted exchange with other ocean basins (Serreze et al., 2007). These factors combine to impart a shelf-derived biogeochemical signature over much of the polar mixed layer, the low salinity surface layer influenced by sea-ice and freshwater, even in the central basin.

In the western Arctic's Canada Basin, hydrographic fronts serve as barriers to rapid shelf-basin exchange processes, thereby eddies and wind-induced upwelling or downwelling constitute the primary mechanisms for off-shelf water and material transport and exchange (Muench et al., 2000; Pickart et al., 2005, 2013). In the eastern Arctic, however, the Transpolar Drift (TPD) is a major current that directly transports shelf water and sea ice directly from the Laptev and East Siberian Seas toward the central basin and Fram Strait, a major outlet for Arctic waters (Ekwurzel et al., 2001; McLaughlin et al., 1996; Rigor et al., 2002; Rudels, 2015; Schlosser et al., 1994). The timescale for the trans-Arctic crossing of this current is on the order of 1-3 years (Pfirman et al., 1997; Steele et al., 2004); as such, the TPD is currently a mechanism for the rapid transport of shelf-derived materials including nutrients and carbon to the deep Arctic basin (Kipp et al., 2018; Letscher et al., 2011; Opsahl et al., 1999; Wheeler et al., 1997), with potential biogeochemical impacts detected as far downstream as the North Atlantic Ocean (e.g. Amon et al., 2003; Gerringa et al., 2015; Noble et al., 2017; Torres-Valdés et al., 2013). At present, primary production in the largely ice-covered central Arctic is light limited; however, surface warming has led to reductions in ice cover, as well as increases in river discharge and permafrost thawing (Frey & McClelland, 2009; McClelland et al., 2004; Peterson et al., 2002; Schuur et al., 2015; Spencer et al.,

2015). With reduced ice cover, the TPD-derived transport of ice-rafted materials might be interrupted (Krumpen et al., 2019), though Newton et al. (2017) have shown that in the near term (~several decades) long distance ice transport will accelerate as the ice thins and is more responsive to the winds. Together, these changes are expected to modify the ecosystem dynamics of the Arctic Ocean, with shelf-basin exchange processes playing a significant role.

In 2015, three nations led cruises to the Arctic Ocean as part of the international GEOTRACES program, a global survey of the distributions of oceanic trace element and isotopes (TEIs). The Arctic GEOTRACES program represented an unprecedented effort in sampling of the Arctic water column from a biogeochemical perspective. High-resolution coverage of waters above 84°N captured the TEI fingerprint of the TPD, and will serve as an important reference for future studies that focus on climate change impacts in the Arctic. Radium isotopes measured during the Arctic GEOTRACES cruises have already been used to show that the chemical composition of the TPD is modified during passage over the Laptev Shelf, and to suggest that potentially significant changes in the flux of nutrients and carbon from the Siberian shelves are already underway (Kadko et al., 2019; Kipp et al., 2018; Rutgers van der Loeff et al., 2018). Additionally, Rijkenberg et al (2018) found higher dissolved Fe and Slagter et al. (2017) found increased concentrations of Fe-binding organic ligands in the path of the TPD relative to adjacent sampling stations. These ligands and the associated Fe on the one hand were found to correlate strongly with terrestrial sources, which are projected to increase in a changing Arctic. On the other hand, Rijkenberg et al (2018) found a local occurrence of Fe limitation over the Nansen basin and hypothesized that retreating ice could further exacerbate this nutrient limitation.

This paper is a synthesis of the distributions of TEIs in the central Arctic Ocean associated with the TPD. We examine the origin and fate of TEIs in this important trans-Arctic conduit and provide a first estimate of the mass transport rate for the TPD, based on

ice drift trajectories and radionuclide tracers. By combining the TPD mass transport estimate with the TEI inventories reported herein, fluxes of these elements to the central Arctic Ocean via the TPD are estimated. Finally, we discuss the biogeochemical implications of the changing climate on TEI concentrations and fluxes to the Arctic and North Atlantic Oceans.

Study Area

The characteristics of water masses in the Arctic Ocean are controlled by bathymetry and inflows from the Atlantic and Pacific Oceans. The Arctic has two major basins, the Eurasian and Amerasian Basins, which are separated by the Lomonosov Ridge (Rudels, 2015). The Lomonosov Ridge is an underwater ridge of continental crust that emerges north of the Siberian shelves at approximately 140°E. Here we refer to the Amerasian Basin as the "western Arctic", while the Siberian shelves and Eurasian Basin are referred to as the "eastern Arctic". The Eurasian Basin is further divided into the Nansen and Amundsen Basins by the Gakkel Ridge, and the Amerasian Basin is divided by the Alpha-Mendeleev Ridge into the large Canada Basin and the Makarov Basin. Surrounding these basins are wide, shallow continental shelves that occupy over 50% of the Arctic Ocean's area (Jakobsson, 2002). Pacific water flows into the Arctic through the narrow and shallow Bering Strait, while Atlantic water enters through the Barents Sea and the Fram Strait (Rudels, 2009). The major outflows of Arctic waters are through the Canadian Arctic Archipelago and Fram Strait, on either side of Greenland, into the North Atlantic (Carmack et al., 2016) (Fig. 1).

Salinity is the largest control on water density, and therefore large-scale pressure gradients, in the Arctic Ocean. Between the (relatively fresh) North Pacific and the (salty) North Atlantic waters, there is a steric height gradient of about a meter, creating a pressure gradient across the Arctic from the Pacific down to the Atlantic. Large inputs of freshwater along the Arctic coastlines create a sea-surface height gradient from the coasts to the central

basins, which drives a series of boundary currents in the coastal seas and over the continental slope that move water eastward (counter-clockwise) around the Arctic (Rudels et al., 1994; Rudels, 2015).

Overprinted on these perennial pressure gradients, the surface circulation is strongly impacted by winds. Predominant atmospheric circulation causes the average sea level pressure to be high over the Canada Basin and low over the Eurasian Basin, Barents Sea, and Nordic Seas (Hunkins & Whitehead, 1992; Serreze & Barrett, 2011). The resulting winds draw relatively fresh water over the Amerasian Basin, and set up the anti-cyclonic Beaufort Gyre, and a weaker cyclonic gyre in the Eurasian Basin (Alkire et al., 2015; Bauch et al., 2011; Carmack et al., 2016; Ekwurzel et al., 2001; Newton et al., 1974; Proshutinsky & Johnson, 1997). These two circulation cells converge just north of Siberia to form the Transpolar Drift (Rudels, 2015). The TPD extends from the Siberian shelves to the Fram Strait, as inferred from ice motion (Rigor et al., 2002) and water mass characteristics (McLaughlin et al., 1996).

The position of the TPD is determined by the Arctic Oscillation (AO), a large-scale Arctic climate pattern characterized by sea level pressure anomalies (Fig. 1). The AO is highly correlated with the North Atlantic Oscillation (NAO) (Mysak, 2001), sea level pressure over the central Arctic, and with sea surface height anomalies along the coastal Arctic (Newton et al., 2006).

During a low or negative AO and NAO, a strong Arctic High exists over the Canada Basin, expanding the anticyclonic Beaufort Gyre. In this case, the TPD originates from the Laptev and East Siberian Seas and flows over the Lomonosov Ridge (Morison et al., 2006; Woodgate et al., 2005) (solid red arrows in Fig. 1). Positive AO and NAO indices produce a weak Arctic High, resulting in a smaller Beaufort Gyre (Mysak, 2001). In a persistently positive phase of the AO, the TPD shifts eastward towards the Bering Strait, entraining more

Pacific water from the Chukchi Sea while still receiving a contribution from the East Siberian Shelf waters, which are transported farther east along the shelf before entering the TPD (Morison et al., 2012; Mysak, 2001) (dashed red arrows in Fig. 1). During the years preceding the 2015 Arctic GEOTRACES sampling, the annual average AO was neutral to negative, and thus during the expeditions the TPD was located over the Lomonosov Ridge (Kipp et al., 2018; Rutgers van der Loeff et al., 2018). Monitoring of atmospheric circulation (Morison et al., 2012; Proshutinsky et al., 2009) as well as biogeochemical and water mass properties on previous hydrographic transects (Falck et al., 2005; Morison et al., 2012; Steele et al., 2004) provide evidence that this position has remained relatively stable over the past ca. 30 years.

The characteristics of the upper water column differ on either side of the TPD because it generally acts as a boundary between Atlantic and Pacific contributions to the Arctic pycnocline. High nutrient, high DOM, low salinity Pacific water is typically observed as an "upper halocline" over the Canada and Makarov Basins, where it separates surface waters from the Atlantic boundary currents below about 200 meters. Sub-surface distributions of nitrate, phosphate and silicate indicate that a layer of nutrient-rich shelf-modified Bering Strait Inflow thins and shoals northward from the Chukchi continental slope and dissipates in the vicinity of the TPD. Pacific influence is dominant in the Canadian Arctic Archipelago (Jones et al., 2003; Jones & Anderson, 2008) and extends north of Greenland to the Fram Strait (Dmitrenko et al., 2019; de Steur et al., 2013). Over the Eurasian Basin, the Pacific-influenced layer is absent, with Atlantic waters occupying the entire water column (Bauch et al., 2011).

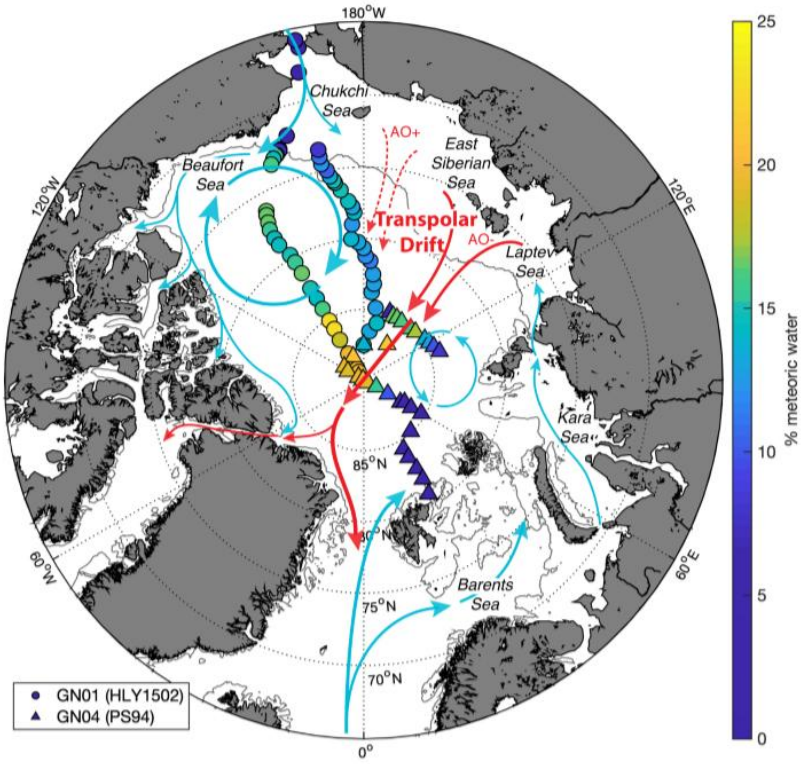

Fig. 1. Map of the Arctic Ocean with the major upper ocean circulation features (blue arrows) as well as the Transpolar Drift (TPD; red arrows). The symbols indicate the station locations for the two GEOTRACES cruises GN01 (circles) and GN04 (triangles). The symbol colors denote the meteoric water fraction at each station. Also shown is the approximate location of the TPD origin for the positive (AO+) and negative (AO-) modes of the Arctic Oscillation (AO). The 200m isobath is shown in grey.

Methods

Sampling and Analyses of TEIs

The data presented herein was collected primarily during two cruises in 2015 associated with the Arctic GEOTRACES program. The U.S. GEOTRACES GN01 (HLY1502) cruise was held aboard the USCGC Healy, while the German GEOTRACES GN04 (PS94) cruise was on the R/V Polarstern (Fig. 1). All sampling and analyses were conducted according to pre-established GEOTRACES approved protocols (for TEIs) (Cutter et al., 2014) and/or GO-SHIP approved protocols (for non-TEIs) (Hood et al., 2010). To

further ensure quality of TEI data across participating laboratories, extensive intercalibration efforts were taken in accordance with GEOTRACES protocols (Cutter, 2013). For example, the GN01 and GN04 cruises both occupied the same station within two weeks of each other (GN01 station 30 and GN04 station 101), which enabled investigators to intercompare results for their respective TEIs. CTD/rosette data and methodologies for PS94 are available via the PANGEA database (Ober et al., 2016a, 2016b; Rabe et al., 2016b, 2016a). The GN01 CTD/rosette procedures are stored on the BCO-DMO database (Landing et al., 2019a, 2019b). Detailed methodologies can be found in the publications where the original TEI data were first reported (in case of Hg: Lamborg et al., 2016, Heimbürge et al., 2015, Agather et al., 2019). The GN01 and GN04 Hg species data were intercalibrated at the crossover station. Total Hg concentrations agreed well for the majority of sampling depths. The tHg and MeHg data have been intercalibrated and validated by the GEOTRACES standards & intercalibration committee.

Linear Mixing Model

In order to study the provenance and pathways of TEIs carried by the TPD, we must quantitatively parse the fraction (f) of source waters in each collected GEOTRACES sample. To do so, we use the relatively well-studied distribution of salinity (S), $\delta^{18}O\text{-}H_2O$ ratios, and the Arctic N-P tracer (ANP; see Newton et al., 2013). These can be used to identify fractions of Pacific (Pac)- and Atlantic (Atl)- sourced sea water, sea-ice melt (SIM), and meteoric water (Met). The latter includes runoff and net in-situ precipitation. Along the cruise transects, in-situ precipitation is expected to be small in comparison with the continental runoff; hence f_{Met} will be our primary proxy for determining the water masses most influenced by the TPD. The value for each in a sample is expressed as a linear combination of the values in its constituent water masses:

$$f_{Atl}[S_{Atl}] + f_{Pac}[S_{Pac}] + f_{Met}[S_{Met}] + f_{SIM}[S_{SIM}] = [S]_{Obs}$$

$$f_{Atl}[\delta^{18}O_{Atl}] + f_{Pac}[\delta^{18}O_{Pac}] + f_{Met}[\delta^{18}O_{Met}] + f_{SIM}[\delta^{18}O_{SIM}] = [\delta^{18}O]_{Obs}$$

$$f_{Atl}[ANP_{Atl}] + f_{Pac}[ANP_{Pac}] + f_{Met}[ANP_{Met}] + f_{SIM}[ANP_{SIM}] = [ANP]_{Obs}$$

$$f_{Atl} + f_{Pac} + f_{Met} + f_{SIM} = 1$$

This constitutes a 4-dimensional linear system that can be solved in matrix form:

$$[f] = \{C\}^{-1}[y],$$

where [f] is a vector of water-mass fractions, [y] is a vector of the parameter values in the sample, and {C} is a matrix of values in the 'end members', i.e. the source waters. The model assumes 4 end members (Table 1) and 4 equations, so will yield an exact solution.

Table 1. Endmember parameter values for the water mass analysis linear mixing model. References: [a] Newton et al. (2013); [b] Pacific Water: slope = 14; intersept = -11; Atlantic Water: slope = 17; intersept = -2.

Water Mass	Salinity	δ^{18}O (‰)	Arctic N : P [a,b]
Atlantic Water	34.92	+0.3	0
Pacific Water	32.50	-1.1	1
Meteoric Water	0	-20	0
Sea-Ice Meltwater	4	Surface +2.6	Surface

There are several important sources of error, which are discussed in detail by Newton et al. (2013) in the context of the 2005 Arctic Ocean Section. Briefly, the least-constrained fractions are those of Pacific- and Atlantic- influenced ocean water, which suffer from the non-conservative nature of nutrients in the ocean, large scatter in the values in the source waters, and potentially from drift in the end-member means with time (Newton et al., 2013). Fortunately, our focus here is on the concentration of meteoric waters and this fraction is

insensitive to nutrient concentrations. Rather, it depends on salinity and $\delta^{18}O$ with the error originating primarily from seasonal and geographical variability in the $\delta^{18}O$ endmember of Arctic rivers (Cooper et al., 2008). Monte Carlo analysis across a reasonable range of estimated mean $\delta^{18}O$ values for runoff yielded errors of about 1% on the meteoric fractions.

The relationship between each TEI and the meteoric water fraction was determined using a linear regression model. The slope, intercept, r^2 value, and p value for each Hg species are reported in Table 2. The effective shelf endmember concentrations of the TEIs were calculated using their respective linear regressions at 20% meteoric water, assuming that this is the meteoric water fraction of the TPD when it leaves the shelf and that there was no significant TEI removal or addition during transport. Meteoric water fractions of 10 – 35% have been observed at the point of origin of the TPD in the Laptev Sea (Bauch et al., 2011) and its terminus at the Fram Strait (Dodd et al., 2012). During the 2015 GEOTRACES expeditions, fractions up to 25% were observed near the North Pole, thus 20% is a conservative estimate.

Table 2. Linear curve fit data and statistics for the Hg species vs. meteoric water relationship plots.

Property	slope	y-int	r2	p
total Hg (pM)	0.0057	1.16	0.00	0.619
total MeHg (pM)	-0.0054	0.16	0.29	0.005
MMHg (pM)	0.0026	0.04	0.07	0.371

Initial estimates of river endmember concentrations were calculated by extrapolating the linear regression to 100% meteoric water (regression intercept). These estimates have a high statistical uncertainty associated with them due to the extrapolation beyond the

measured range and other factors that violate the assumptions of the standard estuarine mixing model (Boyle et al., 1974; Shiller, 1996), but they still provide a first approximation to compare with sparse existing river and shelf sea data. There is some data on TEI concentrations in the Eurasian rivers that ultimately feed into the TPD. Most are derived from the Arctic Great Rivers Observatory (A-GRO), which began as the Pan-Arctic River Transport of Nutrients, Organic Matter and Suspended Sediments (PARTNERS) project (Holmes et al., 2019). The weighted averages reported by the A-GRO provide a useful comparison for many of the elements discussed in this manuscript, but could be improved with measurements of more TEIs in each of the Arctic rivers and knowledge of the relative influence of each river in the TPD at a given time. Due to the shelf circulation patterns (Fig. 1), the major Eurasian rivers (Lena, Ob', Yenisey, and Kolyma) will exert a stronger influence on the TPD than the North American rivers (Mackenzie and Yukon). As such, we report herein the discharge weighted average TEI concentrations for the Eurasian rivers only. Most importantly, any differences between the effective river endmember and the mean river concentrations should not be interpreted in a quantitative manner; rather, this analysis is meant only to give the reader a sense of the relative influence of rivers and/or estuarine removal/addition processes on the TEIs that are transported to the central Arctic Ocean via the TPD.

Results and Discussion

We define the lateral extent of the TPD as ~84°N (in the Canada Basin) to 87°N (in the Eurasian Basin) for waters in the top 50 m. These boundaries were chosen qualitatively based on the distributions of the meteoric water fraction and TPD-influenced TEIs (Fig. 2). For example, there is a sharp concentration gradient for chromophoric dissolved organic matter (CDOM), dissolved organic carbon (DOC), dissolved Fe, and ^{228}Ra at stations north of 84°N 150°W, which coincides with a front between high and intermediate meteoric water

fractions (~250 km along the section distance in Fig. 2). On the Eurasian side of the transect, there is minimal meteoric water influence south of 87°N (~1100 km along the section distance in Fig. 2). The TPD can be characterized generally by this high meteoric water component, which is due to large river contributions to the Siberian Arctic shelves. However, the meteoric water fraction alone cannot be used to delineate the western boundary of the TPD because the Beaufort Gyre in the Canada Basin contains a significant and growing freshwater component sourced from eastern Arctic rivers (Giles et al., 2012; Morison et al., 2012; Rabe et al., 2011, 2014).

As a function of depth, the elevated TEI concentrations and meteoric water fractions are confined to the upper 50 m. The 50 m cutoff also serves to exclude the halocline from our analysis, which is rich in certain TEIs and nutrients like silicate (Fig. 2g), and is influenced by different ventilation processes and source water masses than the TPD (Aagaard et al., 1981). The data presented herein are shown mainly as a function of the meteoric water fraction and were collected in the upper 50 m of the water column for all stations north of 84°N, which includes the polar mixed layer and the TPD.

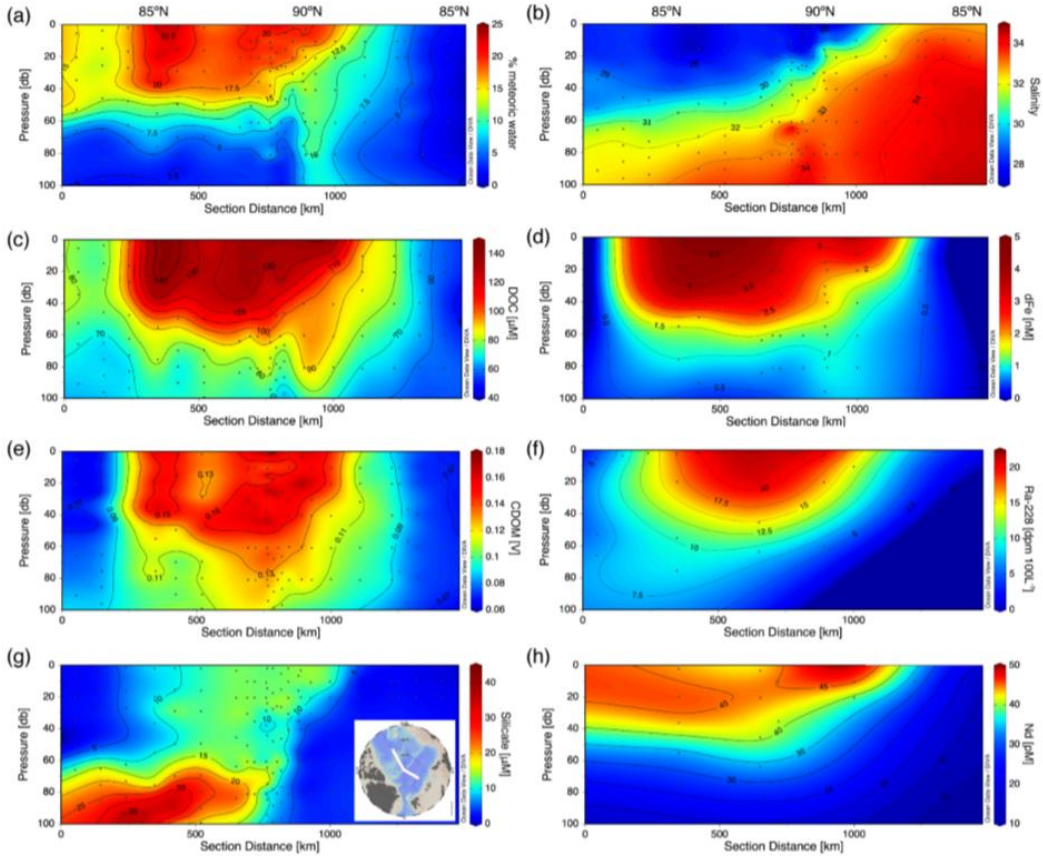

Fig. 2. Section plots for key trace element and isotope concentrations along a transect that spans two GEOTRACES cruises and bisects the Transpolar Drift. The stations included in the contour plots is shown on the map inset for (g) and the distance is relative to a station located at 82°N, 150°W.

Trace Element and Isotope Distributions, Sources, and Sinks

Mercury

Among all stations located north of 84°N and shallower than 50 m, total mercury (tHg) ranged from ~0.5-2.5 pmol L^{-1}, methyl-mercury (MeHg, the sum of mono- and dimethyl-mercury) ranged from <0.05-0.22 pmol L^{-1}, monomethyl-mercury (MMHg) ranged from <0.05-0.20 pmol L^{-1}, and dimethyl-mercury (DMHg) ranged from <0.05-0.12 pmol L^{-1} (Fig. 3).

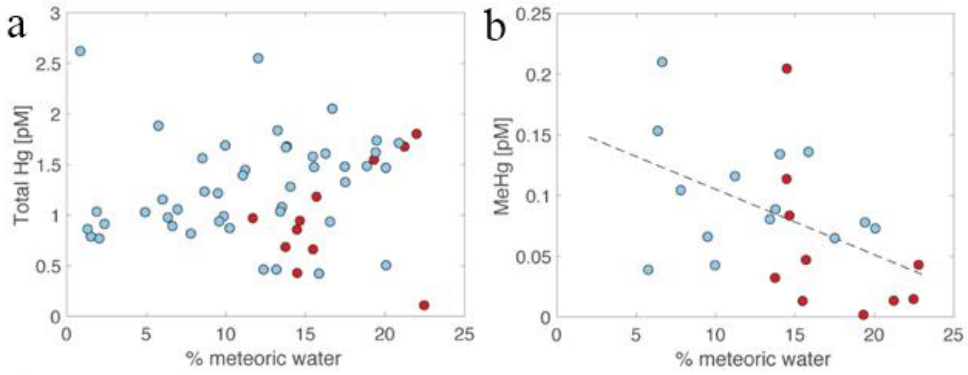

Fig. 3. Total Hg (a) and MeHg (b) concentrations as a function of the meteoric water percentage at stations from the GEOTRACES GN01 (red circles) and GN04 (blue circles) cruises. Data are restricted to 0-50 m for stations north of 84°N. Regression lines are shown for variables with significant ($p<0.05$) relationships with meteoric water.

Contrary to all other open ocean basins, total Hg concentrations were enriched in surface waters. Total Hg and MeHg correspond well to the few previous observations available in the central Arctic Ocean (Heimbürger et al., 2015) and the Canadian Arctic Archipelago (F. Wang et al., 2012; K. Wang et al., 2018): tHg surface enrichment followed by a shallow MeHg peak at the halocline and in the Atlantic waters below. Prior to the 2015 GEOTRACES campaign, there were no MMHg and DMHg data for the central Arctic Ocean. Similar to other open ocean basins, MeHg concentrations were depleted in surface waters, likely due to a combination of MeHg photodemethylation, MMHg uptake into phytoplankton and DMHg evasion to the atmosphere. Although ice can act as a barrier to air-sea gas exchange and hinder elemental Hg (Hg^0) evasion (DiMento et al., 2019), no significant differences were observed between the MeHg concentrations at ice covered versus non-ice covered stations. Looking forward, ice thinning and melting in the central Arctic (Krumpen et al., 2019) may reduce this barrier.

Samples with elevated meteoric water fractions (>15%) were characterized by higher tHg concentrations (up to ~2 pmol L^{-1}), though there was no significant correlation between

the two variables. This might be because rivers are not the only source of tHg to the water column. Mercury also enters the Arctic Ocean via atmospheric deposition and oceanic inputs, mostly from the Atlantic Ocean (Cossa et al., 2018; Outridge et al., 2008; Soerensen et al., 2016; Sonke et al., 2018). However, the lack of correlation between total Hg and meteoric water input in the TPD is surprising given the substantial input flux predicted from measurements of Hg in Arctic rivers. Sonke et al. (2018) derived a discharge-weighted tHg concentration of 46 pmol L^{-1} for the monitored Eurasian rivers, with values of up to 191 pmol L^{-1} in the spring freshet (Yenisei River). This result implies a large loss of Hg in estuaries and shelves, which may be the result of atmospheric evasion (Fisher et al., 2012; Sonke & Heimbürger, 2012). A more recent box model study reveals that a portion of the evading Hg is in the form of DMHg (Soerensen et al., 2016). Estuarine and shelf sediments might also act as sinks for Hg entering from pan-Arctic rivers (e.g., Amos et al., 2014), but this idea remains to be tested for this basin.

The MeHg species had no significant correlation to meteoric water fraction above 84°N. Since shelf sediments can be sources of MeHg (e.g., Hammerschmidt & Fitzgerald, 2006; Hollweg et al., 2010), we might expect a correlation to meteoric water inputs. The lack of such a correlation suggests that either MeHg produced on the Eurasian shelves was lost to demethylation processes during the ~6-18-month transit from the shelf-break to the central Arctic Ocean, or that production in the mixed layer is a stronger source than the shelves. Large subsurface maxima in methylated Hg species (Agather et al., 2019; Heimbürger et al., 2015) suggests a third source for MeHg in the TPD could be diffusion from the MeHg species-rich halocline (Soerensen et al., 2016).

In the future, climate warming is expected to increase Hg inputs to the Arctic drastically as permafrost contains large Hg stocks (Schuster et al., 2018). The Arctic reservoir with the highest relative proportion of MeHg, often representing more than 40%, is generally

open ocean sea water (Heimbürger et al., 2015). It is primarily the ocean-sourced MeHg that bioamplifies to harmful levels, putting Arctic wildlife and human health at risk. The additional input of Hg and DOC might further stimulate MeHg production in the Arctic Ocean. Future coupled ocean-atmosphere numerical models (e.g. Fisher et al., 2012; Zhang et al., 2015) and box model assessments (e.g. Soerensen et al., 2016) designed to constrain Arctic Hg cycling will need to consider Hg cycling and transport associated with the TPD.

Conclusions

Intensification of the hydrologic cycle and permafrost degradation may result in the release of about 25% of the carbon stored in Arctic soils in the next 100 years (Gruber et al., 2004). According to the NOAA Arctic report card (Osborne et al., 2018), the 2018 summer/autumn discharge for the largest rivers flowing into the Arctic was 20% greater than in the 1980-89 period and will continue to increase. These changes will have a substantial effect on the riverine supply of DOM into the Arctic Ocean, as well as the long-distance transport of TEIs within the Transpolar Drift that are likely complexed by this organic matter, including Fe, Co, Ni, Cu, Th, and possibly the REEs.

While the halocline contains ample nutrient concentrations, the increased freshwater inputs are strengthening water column stratification, which could further limit nutrient inputs via vertical mixing processes (Rudels et al., 1991). Hence, increased macro- and micro-nutrient concentrations delivered to the central Arctic Ocean via the TPD may play an important role in upper ocean productivity in the coming decades, since, for example, nitrate already limits primary production in some Arctic locations (Tremblay & Gagnon, 2009), as does Fe in the case of one large under ice bloom (Rijkenberg et al., 2018). In the case of Fe, whether limitation will occur in the changing Arctic will depend on the interplay between nutrient utilization ratios (Rijkenberg et al., 2018) and projected increases of ligand-borne, specifically humic-borne, terrestrial dFe (Slagter et al., 2017, 2019).

The complexity of physical and biochemical factors and their interplay, such as the effect of increased river runoff and stratification on the saturation state of aragonite (Yamamoto-Kawai et al., 2009), combine with scarcity of data to make future effects of TPD influence on the central Arctic difficult to predict (Carmack & McLaughlin, 2011). However, DOM is strongly related to hydrographic parameters and biogeochemical cycles in the shelf seas and TPD (Amon et al., 2003; Granskog et al., 2012), but has the advantage of relatively simple measurement via remote sensing in ice-free waters (Fichot et al., 2013; Juhls et al., 2019; Matsuoka et al., 2017) or in-situ instrumentation capable of high vertical resolution such as the fluorometers deployed on these cruises. Looking to the future, this makes CDOM a powerful tracer of climate change impacts on a multitude of Arctic system processes (e.g. Stedmon et al., 2015).

For some TEIs, the sediments within the broad and shallow eastern Arctic shelves play a dominant role in their cycling and signature within the TPD. Radium isotopic ratios and a mass balance calculation point to shelf sediments as the dominant source of ^{228}Ra carried by the TPD (Kipp et al., 2018). While ^{228}Ra is not a biologically important TEI, it acts as a quasi-conservative tracer of other shelf-derived materials like Ba, which has TPD concentrations that cannot be fully explained by a river source. The Ra-derived evidence of active sediment-water exchange processes in the eastern Arctic coastal zone supports the apparent strong sinks for Pb and V, which are known to be removed by particle scavenging and/or reduction processes in shelf sediments. Increased ^{228}Ra levels in the TPD therefore suggest that the concentrations of these other TEIs may be affected both positively (Ba) or negatively (Pb, Al, Ga, and V) under a changing climate where shelf sediments are exposed to wind-driven mixing under reduced ice cover.

The TEIs that have the strongest correlation with meteoric water fraction are those that are known to form complexes with organic matter. As a result, other than dilution via

mixing, their concentrations, which are significantly elevated relative to other ocean basins, are preserved in the TPD over distances >1000 km and timescales of up to 18 months. It is therefore reasonable to expect that this TEI "fingerprint" of the TPD would be carried beyond the ice covered central Arctic Ocean, through Fram Strait, and into the ice-free surface waters of the North Atlantic Ocean as seen for Arctic river DOM (Amon et al., 2003; Benner et al., 2005; Granskog et al., 2012). In the present day, the TEIs transported in the TPD may become participants in biogeochemical processes of this ocean basin, or in the future be utilized closer to their source as the pan-Arctic ice cover is reduced with warming temperatures. This new utilization would apply to an increasingly ice-free Arctic Ocean including the Canada Basin, where the Beaufort Gyre (Fig. 1) is known to entrain and store an increasing amount of freshwater sourced from eastern Arctic rivers (Giles et al., 2012; Morison et al., 2012; Rabe et al., 2011, 2014).

Lastly, our understanding of the effects of the changing climate on Arctic Ocean TEI concentrations and fluxes has been greatly hampered by a lack of data, mainly due to the logistics and expense of conducting oceanography at high-latitudes where icebreakers are required for sampling. Geopolitical issues have resulted in large data gaps for the eastern Arctic shelf seas. In the near future, international collaboration through long term observatories at key locations and Arctic gateways, synoptic surveys (e.g. http://www.synopticarcticsurvey.info) and advances in technology (e.g. floats, gliders, ice tethered sensors and samplers) may provide the temporal and spatial coverage needed to address some of the pressing unanswered questions posed herein.

Acknowledgements

This study would not have been possible without the dedication of the captains and crews of the USCGC Healy and R/V Polarstern. The authors also thank the many members of the shipboard scientific parties, including the chief scientists, who enabled sample collection via the various CTD rosette and in situ pumping systems, as well as the sample analyses on the ship and back in their home laboratories. Funding for Arctic GEOTRACES was provided by the U.S. National Science Foundation, Swedish Research Council Formas, French Agence Nationale de la Recherche and LabexMER, Netherlands Organization for Scientific Research, and Independent Research Fund Denmark.

Data from GEOTRACES cruises GN01 (HLY1502) and GN04 (PS94) have been archived at the Biological & Chemical Oceanography Data Management Office (BCO-DMO; https://www.bco-dmo.org/deployment/638807) and PANGAEA (https://www.pangaea.de/?q=PS94&f.campaign%5B%5D=PS94) websites, respectively. The inorganic carbon data are available at the NOAA Ocean Carbon Data System (OCADS; doi:10.3334/CDIAC/OTG.CLIVAR_ARC01_33HQ20150809).

References

Aagaard, K., Coachman, L. K., & Carmack, E., 1981. On the halocline of the Arctic Ocean. Deep Sea Research Part A, Oceanographic Research Papers, 28(6), 529–545

Abbott, A. N., Haley, B. A., McManus, J., & Reimers, C. E., 2015. The sedimentary flux of dissolved rare earth elements to the ocean. Geochimica et Cosmochimica Acta, 154, 186–200

Agather, A. M., Bowman, K. L., Lamborg, C. H., & Hammerschmidt, C. R., 2019. Distribution of mercury species in the Western Arctic Ocean (U.S. GEOTRACES GN01). Marine Chemistry, 216, 103686

Alkire, M. B., Morison, J., & Andersen, R., 2015. Variability in the meteoric water, sea-ice melt, and Pacific water contributions to the central Arctic Ocean, 2000-2014. Journal of Geophysical Research: Oceans, 120(3), 1573–1598

Amon, R. M. W., Budéus, G., & Meon, B., 2003. Dissolved organic carbon distribution and origin in the Nordic Seas: Exchanges with the Arctic Oean and the North Atlantic. Journal of Geophysical Research C: Oceans, 108(C7), 1–17

Amos, H. M., Jacob, D. J., Kocman, D., Horowitz, H. M., Zhang, Y., Dutkiewicz, S., et al., 2014. Global biogeochemical implications of mercury discharges from rivers and sediment burial. Environmental Science and Technology, 48(16), 9514–9522

Anderson, R. F., Cheng, H., Edwards, R. L., Fleisher, M. Q., Hayes, C. T., Huang, K. F., et al., 2016. How well can we quantify dust deposition to the ocean? Philosophical Transactions of the Royal Society A: Mathematical, Physical and Engineering Sciences, 374(2081), 20150285

Arsouze, T., Dutay, J.-C., Lacan, F., & Jeandel, C., 2009. Reconstructing the Nd oceanic cycle using a coupled dynamical – biogeochemical model. Biogeosciences, 6(12), 2829–2846

Bauch, D., van der Loeff, M. R., Andersen, N., Torres-Valdes, S., Bakker, K., & Abrahamsen, E. P., 2011. Origin of freshwater and polynya water in the Arctic Ocean halocline in summer 2007. Progress in Oceanography, 91(4), 482–495

Benner, R., Louchouarn, P., & Amon, R. M. W., 2005. Terrigenous dissolved organic matter in the Arctic Ocean and its transport to surface and deep waters of the North Atlantic. Global Biogeochemical Cycles, 19(2), 1–11

Boyle, E., Collier, R., Dengler, A. T., Edmond, J. M., Ng, A. C., & Stallard, R. F., 1974. On the chemical mass-balance in estuaries. Geochimica et Cosmochimica Acta, 38(11), 1719–1728

Cameron, V., & Vance, D., 2014. Heavy nickel isotope compositions in rivers and the oceans. Geochimica et Cosmochimica Acta, 128, 195–211

Carmack, E. C., & McLaughlin, F., 2011. Towards recognition of physical and geochemical change in Subarctic and Arctic Seas. Progress in Oceanography, 90(1–4), 90–104

Carmack, E. C., Yamamoto-Kawai, M., Haine, T. W. N., Bacon, S., Bluhm, B. A., Lique, C., et al., 2016. Freshwater and its role in the Arctic Marine System: Sources, disposition, storage, export, and physical and biogeochemical consequences in the Arctic and global oceans. Journal of Geophysical Research G: Biogeosciences, 121(3), 675–717

Cooper, L. W., McClelland, J. W., Holmes, R. M., Raymond, P. A., Gibson, J. J., Guay, C. K., & Peterson, B. J., 2008. Flow-weighted values of runoff tracers (δ18O, DOC, Ba, alkalinity) from the six largest Arctic rivers. Geophysical Research Letters, 35(18), L18606

Cossa, D., Heimbürger, L. E., Pérez, F. F., García-Ibáñez, M. I., Sonke, J. E., Planquette, H., et al., 2018. Mercury distribution and transport in the North Atlantic Ocean along the GEOTRACES-GA01 transect. Biogeosciences, 15(8), 2309–2323

Cutter, G. A., 2013. Intercalibration in chemical oceanography-Getting the right number. Limnology and Oceanography: Methods, 11(JULY), 418–424

Cutter, G. A., Andersson, P. S., Codispoti, L., Croot, P. L., Francois, R., Lohan, M. C., et al., 2014. Sampling and Sample-handing Protocols for GEOTRACES Cruises. Retrieved from http://www.geotraces.org/images/stories/documents/intercalibration/Cookbook_v2.pdf

DiMento, B. P., Mason, R. P., Brooks, S., & Moore, C., 2019. The impact of sea ice on the air-sea exchange of mercury in the Arctic Ocean. Deep-Sea Research Part I: Oceanographic Research Papers, 144, 28–38

Dmitrenko, I. A., Kirillov, S. A., Rudels, B., Babb, D. G., Myers, P. G., Stedmon, C. A., et al., 2019. Variability of the Pacific-Derived Arctic Water Over the Southeastern Wandel Sea Shelf (Northeast Greenland) in 2015–2016. Journal of Geophysical Research: Oceans, 124(1), 349–373

Dodd, P. A., Rabe, B., Hansen, E., Falck, E., MacKensen, A., Rohling, E., et al., 2012. The freshwater composition of the Fram Strait outflow derived from a decade of tracer measurements. Journal of Geophysical Research: Oceans, 117(11), C11005

Ekwurzel, B., Schlosser, P., Mortlock, R. A., Fairbanks, R. G., & Swift, J. H., 2001. River runoff, sea ice meltwater, and Pacific water distribution and mean residence times in the Arctic Ocean. Journal of Geophysical Research: Oceans, 106(C5), 9075–9092

Falck, E., Kattner, G., & Budéus, G., 2005. Disappearance of Pacific Water in the northwestern Fram Strait. Geophysical Research Letters, 32(14), 1–4

Fichot, C. G., Kaiser, K., Hooker, S. B., Amon, R. M. W., Babin, M., Bélanger, S., et al., 2013. Pan-Arctic distributions of continental runoff in the Arctic Ocean. Scientific Reports, 3(1053), 1–6

Fisher, J. A., Jacob, D. J., Soerensen, A. L., Amos, H. M., Steffen, A., & Sunderland,

E. M., 2012. Riverine source of Arctic Ocean mercury inferred from atmospheric observations. Nature Geoscience, 5(7), 499–504

Frey, K. E., & McClelland, J. W., 2009. Impacts of permafrost degradation on arctic river biogeochemistry. Hydrological Processes, 23(1), 169–182

Gerringa, L. J. A., Rijkenberg, M. J. A., Schoemann, V., Laan, P., & de Baar, H. J. W., 2015. Organic complexation of iron in the West Atlantic Ocean. Marine Chemistry, 177, 434–446

Giles, K. A., Laxon, S. W., Ridout, A. L., Wingham, D. J., & Bacon, S., 2012. Western Arctic Ocean freshwater storage increased by wind-driven spin-up of the Beaufort Gyre. Nature Geoscience, 5(3), 194–197

Granskog, M. A., Stedmon, C. A., Dodd, P. A., Amon, R. M. W., Pavlov, A. K., De Steur, L., & Hansen, E., 2012. Characteristics of colored dissolved organic matter (CDOM) in the Arctic outflow in the Fram Strait: Assessing the changes and fate of terrigenous CDOM in the Arctic Ocean. Journal of Geophysical Research: Oceans, 117(12), C12021

Gruber, N., Friedlingstein, P., Field, C., Valentini, R., Heimann, M., Richey, J., et al., 2004. The vulnerability of the carbon cycle in the 21st century: an assessment of carbon-climate-human interactions. In C. B. Field & M. R. Raupach (Eds.), Toward CO2 Stabilization: Issues, Strategies, and Consequences (pp. 45–76). Washington, DC: Island Press.

Hammerschmidt, C. R., & Fitzgerald, W. F., 2006. Methylmercury cycling in sediments on the continental shelf of southern New England. Geochimica et Cosmochimica Acta, 70(4), 918–930

Hayes, C. T., Anderson, R. F., Fleisher, M. Q., Serno, S., Winckler, G., & Gersonde, R., 2013. Quantifying lithogenic inputs to the North Pacific Ocean using the long-lived thorium isotopes. Earth and Planetary Science Letters, 383, 16–25

Heimbürger, L. E., Sonke, J. E., Cossa, D., Point, D., Lagane, C., Laffont, L., et al., 2015. Shallow methylmercury production in the marginal sea ice zone of the central Arctic Ocean. Scientific Reports, 5(1), 10318

Hollweg, T. A., Gilmour, C. C., & Mason, R. P., 2010. Mercury and methylmercury cycling in sediments of the mid-Atlantic continental shelf and slope. Limnology and Oceanography, 55(6), 2703–2722

Holmes, R. M., McClelland, J. W., Tank, S. E., Spencer, R. G. M., & Shiklomanov, A. I., 2019. Arctic Great Rivers Observatory. Water Quality Dataset, Version 20190904. Retrieved from https://arcticgreatrivers.org/data

Hood, E. M., Sabine, C. L., & Sloyan, B. M. (Eds.)., 2010. The GO-SHIP Repeat Hydrography Manual: A Collection of Expert Reports and Guidelines. IOCCP Report Number 14, ICPO Publication Series Number 134. Retrieved from http://www.go-ship.org/HydroMan.html

Hsieh, Y.-T., Henderson, G. M., & Thomas, A. L., 2011. Combining seawater 232Th and 230Th concentrations to determine dust fluxes to the surface ocean. Earth and Planetary Science Letters, 312(3–4), 280–290

Hunkins, K., & Whitehead, J. A., 1992. Laboratory simulation of exchange through Fram Strait. Journal of Geophysical Research, 97(C7), 299–310

Jakobsson, M., 2002. Hypsometry and volume of the Arctic Ocean and its constituent seas. Geochemistry, Geophysics, Geosystems, 3(5), 1–18

Jones, E. P., & Anderson, L. G., 2008. Is the global conveyor belt threatened by arctic ocean fresh water outflow? In Arctic-Subarctic Ocean Fluxes: Defining the Role of the Northern Seas in Climate (pp. 385–404). Dordrecht: Springer Netherlands

Jones, E. P., Swift, J. H., Anderson, L. G., Lipizer, M., Civitarese, G., Falkner, K. K., et al., 2003. Tracing Pacific water in the North Atlantic Ocean. Journal of Geophysical

Research, 108(C4), 3116

Juhls, B., Paul Overduin, P., Hölemann, J., Hieronymi, M., Matsuoka, A., Heim, B., & Fischer, J., 2019. Dissolved organic matter at the fluvial-marine transition in the Laptev Sea using in situ data and ocean colour remote sensing. Biogeosciences, 16(13), 2693–2713

Kadko, D., Galfond, B., Landing, W. M., & Shelley, R. U., 2016. Determining the pathways, fate, and flux of atmospherically derived trace elements in the Arctic Ocean/ice system. Marine Chemistry, 182, 38–50

Kadko, D., Aguilar-Islas, A., Bolt, C., Buck, C. S., Fitzsimmons, J. N., Jensen, L. T., et al., 2019. The residence times of trace elements determined in the surface Arctic Ocean during the 2015 US Arctic GEOTRACES expedition. Marine Chemistry, 208, 56–69

Kienast, S. S., Winckler, G., Lippold, J., Albani, S., & Mahowald, N. M., 2016. Tracing dust input to the global ocean using thorium isotopes in marine sediments: ThoroMap. Global Biogeochemical Cycles, 30(10), 1526–1541

Kipp, L. E., 2018. Radium isotopes as tracers of boundary inputs of nutrients and trace elements to the coastal and open ocean. Thesis. Massachusetts Institute of Technology

Kipp, L. E., Charette, M. A., Moore, W. S., Henderson, P. B., & Rigor, I. G., 2018. Increased fluxes of shelf-derived materials to the central Arctic Ocean. Science Advances, 4(1), 1–10

Krumpen, T., Belter, H. J., Boetius, A., Damm, E., Haas, C., Hendricks, S., et al., 2019. Arctic warming interrupts the Transpolar Drift and affects long-range transport of sea ice and ice-rafted matter. Scientific Reports, 9(1), 5459

Lammers, R. B., Shiklomanov, A. I., Vörösmarty, C. J., Fekete, B. M., & Peterson, B. J., 2001. Assessment of contemporary Arctic river runoff based on observational discharge records. Journal of Geophysical Research Atmospheres, 106(D4), 3321–3334

Landing, W. M., Cutter, G., & Kadko, D. C., 2019a. Bottle data from the CTD-ODF

carousel on the GEOTRACES Arctic Section cruise (HLY1502) from August to October 2015 (U.S. GEOTRACES Arctic project). Biological and Chemical Oceanography Data Management Office (BCO-DMO)

Landing, W. M., Cutter, G., & Kadko, D. C., 2019b. Bottle data from the GEOTRACES Clean Carousel sampling system (GTC) on the Arctic Section cruise (HLY1502) from August to October 2015 (U.S. GEOTRACES Arctic project). Biological and Chemical Oceanography Data Management Office (BCO-DMO)

Letscher, R. T., Hansell, D. A., & Kadko, D., 2011. Rapid removal of terrigenous dissolved organic carbon over the Eurasian shelves of the Arctic Ocean. Marine Chemistry, 123(1–4), 78–87

Matsuoka, A., Boss, E., Babin, M., Karp-Boss, L., Hafez, M., Chekalyuk, A., et al., 2017. Pan-Arctic optical characteristics of colored dissolved organic matter: Tracing dissolved organic carbon in changing Arctic waters using satellite ocean color data. Remote Sensing of Environment, 200, 89–101

McClelland, J. W., Holmes, R. M., Peterson, B. J., & Stieglitz, M., 2004. Increasing river discharge in the Eurasian Arctic: Consideration of dams, permafrost thaw, and fires as potential agents of change. Journal of Geophysical Research, 109(D18), D18102

McLaughlin, F. A., Carmack, E. C., Macdonald, R. W., & Bishop, J. K. B., 1996. Physical and geochemical properties across the Atlantic/Pacific water mass front in the southern Canadian Basin. Journal of Geophysical Research: Oceans, 101(C1), 1183–1197

Morison, J., Steele, M., Kikuchi, T., Falkner, K., & Smethie, W., 2006. Relaxation of central Arctic Ocean hydrography to pre-1990s climatology. Geophysical Research Letters, 33(17), L17604

Morison, J., Kwok, R., Peralta-Ferriz, C., Alkire, M., Rigor, I., Andersen, R., & Steele, M., 2012. Changing Arctic Ocean freshwater pathways. Nature, 481(7379), 66–70

Muench, R. D., Gunn, J. T., Whitledge, T. E., Schlosser, P., & Smethie, W., 2000. An Arctic Ocean cold core eddy. Journal of Geophysical Research: Oceans, 105(C10), 23997–24006

Mysak, L. A., 2001. Patterns of Arctic Circulation. Science, 293(5533), 1269–1270.

Newton, B., Tremblay, L. B., Cane, M. A., & Schlosser, P., 2006. A simple model of the Arctic Ocean response to annular atmospheric modes. Journal of Geophysical Research: Oceans, 111(9), C09019

Newton, J. L., Aagaard, K., & Coachman, L. K., 1974. Baroclinic eddies in the Arctic Ocean. Deep Sea Research and Oceanographic Abstracts, 21(9), 707–719

Newton, R., Schlosser, P., Mortlock, R., Swift, J., & MacDonald, R., 2013. Canadian Basin freshwater sources and changes: Results from the 2005 Arctic Ocean Section. Journal of Geophysical Research: Oceans, 118(4), 2133–2154

Newton, R., Pfirman, S., Tremblay, B., & DeRepentigny, P., 2017. Increasing transnational sea-ice exchange in a changing Arctic Ocean. Earth's Future, 5(6), 633–647

Noble, A. E., Ohnemus, D. C., Hawco, N. J., Lam, P. J., & Saito, M. A., 2017. Coastal sources, sinks and strong organic complexation of dissolved cobalt within the US North Atlantic GEOTRACES transect GA03. Biogeosciences, 14(11), 2715–2739

Ober, S., Rijkenberg, M. J. A., & Gerringa, L. J. A,. 2016a. Physical oceanography measured with ultra clean CTD/Water sampler-system during POLARSTERN cruise PS94 (ARK-XXIX/3). Royal Netherlands Institute for Sea Research, Texel. PANGEA

Ober, S., Rijkenberg, M. J. A., & Gerringa, L. J. A., 2016b, April 13. Physical oceanography measured on water bottle samples with ultra clean CTD/Water sampler-system during POLARSTERN cruise PS94 (ARK-XXIX/3). Royal Netherlands Institute for Sea Research, Texel. PANGAEA

Opsahl, S., Benner, R., & Amon, R. M. W., 1999. Major flux of terrigenous dissolved

organic matter through the Arctic Ocean. Limnology and Oceanography, 44(8), 2017–2023

Osborne, E., Richter-Menge, J., & Jeffries, M., 2018. Arctic Report Card 2018. Retrieved from https://www.arctic.noaa.gov/Report-Card

Outridge, P. M., Macdonald, R. W., Wang, F., Stern, G. A., & Dastoor, A. P., 2008. A mass balance inventory of mercury in the Arctic Ocean. Environmental Chemistry, 5(2), 89

Peterson, B. J., Holmes, R. M., McClelland, J. W., Vörösmarty, C. J., Lammers, R. B., Shiklomanov, A. I., et al., 2002. Increasing river discharge to the Arctic Ocean. Science, 298(5601), 2171–2173

Pfirman, S. L., Kögeler, J. W., & Rigor, I., 1997. Potential for rapid transport of contaminants from the Kara Sea. Science of The Total Environment, 202(1–3), 111–122

Pickart, R. S., Weingartner, T. J., Pratt, L. J., Zimmermann, S., & Torres, D. J., 2005. Flow of winter-transformed Pacific water into the Western Arctic. Deep Sea Research Part II: Topical Studies in Oceanography, 52(24–26), 3175–3198

Pickart, R. S., Spall, M. A., & Mathis, J. T., 2013. Dynamics of upwelling in the Alaskan Beaufort Sea and associated shelf–basin fluxes. Deep Sea Research Part I: Oceanographic Research Papers, 76, 35–51

Proshutinsky, A. Y., & Johnson, M. A., 1997. Two circulation regimes of the wind-driven Arctic Ocean. Journal of Geophysical Research: Oceans, 102(C6), 12493–12514

Proshutinsky, A. Y., Krishfield, R., Timmermans, M.-L., Toole, J., Carmack, E., McLaughlin, F., et al., 2009. Beaufort Gyre freshwater reservoir: State and variability from observations. Journal of Geophysical Research, 114, C00A10

Rabe, B., Karcher, M., Schauer, U., Toole, J. M., Krishfield, R. A., Pisarev, S., et al., 2011. An assessment of Arctic Ocean freshwater content changes from the 1990s to the 2006-2008 period. Deep-Sea Research Part I: Oceanographic Research Papers, 58(2), 173–185

Rabe, B., Karcher, M., Kauker, F., Schauer, U., Toole, J. M., Krishfield, R. A., et al.,

2014. Arctic Ocean basin liquid freshwater storage trend 1992-2012. Geophysical Research Letters, 41(3), 961–968

Rabe, B., Schauer, U., Ober, S., Horn, M., Hoppmann, M., Korhonen, M., et al., 2016a, April 1). Physical oceanography during POLARSTERN cruise PS94 (ARK-XXIX/3). Alfred Wegener Institute, Helmholtz Centre for Polar and Marine Research, Bremerhaven. PANGAEA

Rabe, B., Schauer, U., Ober, S., Horn, M., Hoppmann, M., Korhonen, M., et al., 2016b, April 13. Physical oceanography measured on water bottle samples during POLARSTERN cruise PS94 (ARK-XXIX/3). Alfred Wegener Institute, Helmholtz Centre for Polar and Marine Research, Bremerhaven. PANGAEA

Raymond, P. A., McClelland, J. W., Holmes, R. M., Zhulidov, A. V., Mull, K., Peterson, B. J., et al., 2007. Flux and age of dissolved organic carbon exported to the Arctic Ocean: A carbon isotopic study of the five largest arctic rivers. Global Biogeochemical Cycles, 21(4), GB4011

Rigor, I. G., Wallace, J. M., & Colony, R. L., 2002. Response of Sea Ice to the Arctic Oscillation. Journal of Climate, 15(18), 2648–2663

Rijkenberg, M. J. A., Slagter, H. A., van der Loeff, M. R., van Ooijen, J., & Gerringa, L. J. A., 2018. Dissolved Fe in the deep and upper Arctic Ocean with a focus on Fe Limitation in the Nansen Basin. Frontiers in Marine Science, 5, 88

Robinson, L. F., Noble, T. L., & McManus, J. F., 2008. Measurement of adsorbed and total 232Th/230Th ratios from marine sediments. Chemical Geology, 252(3–4), 169–179

Rudels, B., 2009. Arctic Ocean Circulation. Encyclopedia of Ocean Sciences, 211–225

Rudels, B., 2015. Arctic Ocean circulation, processes and water masses: A description of observations and ideas with focus on the period prior to the International Polar Year 2007-

2009. Progress in Oceanography, 132, 22–67

Rudels, B., Larsson, A. M., & Sehlstedt, P. I., 1999. Stratification and water mass formation in the Arctic Ocean: some implications for the nutrient distribution. Polar Research, 10(1), 19–32

Rudels, B., Jones, E. P., Anderson, L. G., & Kattner, G. 1994. On the Intermediate Depth Waters of the Arctic Ocean. In The Polar Oceans and Their Role in Shaping the Global Environment (Vol. 85, pp. 33–46). American Geophysical Union

Rutgers van der Loeff, M., Kipp, L., Charette, M. A., Moore, W. S., Black, E., Stimac, I., et al., 2018. Radium Isotopes Across the Arctic Ocean Show Time Scales of Water Mass Ventilation and Increasing Shelf Inputs. Journal of Geophysical Research: Oceans, 123(7), 4853–4873

Schlosser, P., Bauch, D., Fairbanks, R., & Bönisch, G., 1994. Arctic river-runoff: mean residence time on the shelves and in the halocline. Deep Sea Research Part I: Oceanographic Research Papers, 41(7), 1053–1068

Schuster, P. F., Schaefer, K. M., Aiken, G. R., Antweiler, R. C., Dewild, J. F., Gryziec, J. D., et al., 2018. Permafrost Stores a Globally Significant Amount of Mercury. Geophysical Research Letters, 45(3), 1463–1471

Schuur, E. A. G., McGuire, A. D., Schädel, C., Grosse, G., Harden, J. W., Hayes, D. J., et al., 2015. Climate change and the permafrost carbon feedback. Nature, 520, 171–179

Serreze, M. C., & Barrett, A. P., 2011. Characteristics of the Beaufort Sea high. Journal of Climate, 24(1), 159–182

Serreze, M. C., Barrett, A. P., Slater, A. G., Woodgate, R. A., Aagaard, K., Lammers, R. B., et al., 2006. The large-scale freshwater cycle of the Arctic. Journal of Geophysical Research: Oceans, 111(11), C11010

Serreze, M. C., Holland, M. M., & Stroeve, J., 2007. Perspectives on the Arctic's

shrinking sea-ice cover. Science, 315(5818), 1533–6

Shiller, A. M., 1996. The effect of recycling traps and upwelling on estuarine chemical flux estimates. Geochimica et Cosmochimica Acta, 60(17), 3177–3185

Slagter, H. A., Reader, H. E., Rijkenberg, M. J. A., Rutgers van der Loeff, M., de Baar, H. J. W., & Gerringa, L. J. A., 2017. Organic Fe speciation in the Eurasian Basins of the Arctic Ocean and its relation to terrestrial DOM. Marine Chemistry, 197, 11–25

Slagter, H. A., Laglera, L. M., Sukekava, C., & Gerringa, L. J. A., 2019. Fe-Binding Organic Ligands in the Humic-Rich TransPolar Drift in the Surface Arctic Ocean Using Multiple Voltammetric Methods. Journal of Geophysical Research: Oceans, 124(3), 1491–1508

Soerensen, A. L., Jacob, D. J., Schartup, A. T., Fisher, J. A., Lehnherr, I., St Louis, V. L., et al., 2016. A mass budget for mercury and methylmercury in the Arctic Ocean. Global Biogeochemical Cycles, 30(4), 560–575

Sonke, J. E., & Heimbürger, L. E., 2012. Environmental science: Mercury in flux. Nature Geoscience

Sonke, J. E., Teisserenc, R., Heimbürger-Boavida, L.-E., Petrova, M. V, Marusczak, N., Le Dantec, T., et al., 2018. Eurasian river spring flood observations support net Arctic Ocean mercury export to the atmosphere and Atlantic Ocean. Proceedings of the National Academy of Sciences, 115(50), E11586–E11594

Spencer, R. G. M., Mann, P. J., Dittmar, T., Eglinton, T. I., McIntyre, C., Holmes, R. M., et al., 2015. Detecting the signature of permafrost thaw in Arctic rivers. Geophysical Research Letters, 42(8), 2830–2835

Stedmon, C. A., Granskog, M. A., & Dodd, P. A., 2015. An approach to estimate the freshwater contribution from glacial melt and precipitation in East Greenland shelf waters using colored dissolved organic matter (CDOM). Journal of Geophysical Research: Oceans,

120(2), 1107–1117

Steele, M., Morison, J., Ermold, W., Rigor, I., & Ortmeyer, M., 2004. Circulation of summer Pacific halocline water in the Arctic Ocean. Journal of Geophysical Research, 109(C2), C02027

de Steur, L., Steele, M., Hansen, E., Morison, J., Polyakov, I., Olsen, S. M., et al., 2013. Hydrographic changes in the Lincoln Sea in the Arctic Ocean with focus on an upper ocean freshwater anomaly between 2007 and 2010. Journal of Geophysical Research: Oceans, 118(9), 4699–4715

Sunderland, E. M., Mason, R.P., 2007. Human impacts on open ocean mercury concentrations, Global Biogeochem. Cycles,21, GB4022

Torres-Valdés, S., Tsubouchi, T., Bacon, S., Naveira-Garabato, A. C., Sanders, R., McLaughlin, F. A., et al., 2013. Export of nutrients from the Arctic Ocean. Journal of Geophysical Research: Oceans, 118(4), 1625–1644

Tremblay, J.-É., & Gagnon, J., 2009. The effects of irradiance and nutrient supply on the productivity of Arctic waters: a perspective on climate change. In Influence of Climate Change on the Changing Arctic and Sub-Arctic Conditions (pp. 73–93). Dordrecht: Springer Netherlands

Vieira, L. H., Achterberg, E. P., Scholten, J., Beck, A. J., Liebetrau, V., Mills, M. M., & Arrigo, K. R., 2019. Benthic fluxes of trace metals in the Chukchi Sea and their transport into the Arctic Ocean. Marine Chemistry, 208, 43–55

Wang, F., Macdonald, R. W., Armstrong, D. A., & Stern, G. A., 2012. Total and Methylated Mercury in the Beaufort Sea: The Role of Local and Recent Organic Remineralization. Environmental Science & Technology, 46(21), 11821–11828

Wang, K., Munson, K. M., Beaupré-Laperrière, A., Mucci, A., Macdonald, R. W., & Wang, F., 2018. Subsurface seawater methylmercury maximum explains biotic mercury

concentrations in the Canadian Arctic. Scientific Reports, 8(1), 14465

Wheeler, P. A., Watkins, J. M., & Hansing, R. L., 1997. Nutrients, organic carbon and organic nitrogen in the upper water column of the Arctic Ocean: implications for the sources of dissolved organic carbon. Deep Sea Research Part II: Topical Studies in Oceanography, 44(8), 1571–1592

Woodgate, R. A., Aagaard, K., & Weingartner, T. J., 2005. A year in the physical oceanography of the Chukchi Sea: Moored measurements from autumn 1990-1991. Deep-Sea Research Part II: Topical Studies in Oceanography, 52(24–26), 3116–3149

Yamamoto-Kawai, M., McLaughlin, F. A., Carmack, E. C., Nishino, S., & Shimada, K., 2009. Aragonite undersaturation in the Arctic Ocean: effects of ocean acidification and sea ice melt. Science, 326(5956), 1098–100

Zhang, Y., Jacob, D. J., Dutkiewicz, S., Amos, H. M., Long, M. S., & Sunderland, E. M., 2015. Biogeochemical drivers of the fate of riverine mercury discharged to the global and Arctic oceans. Global Biogeochemical Cycles, 29(6), 854–864